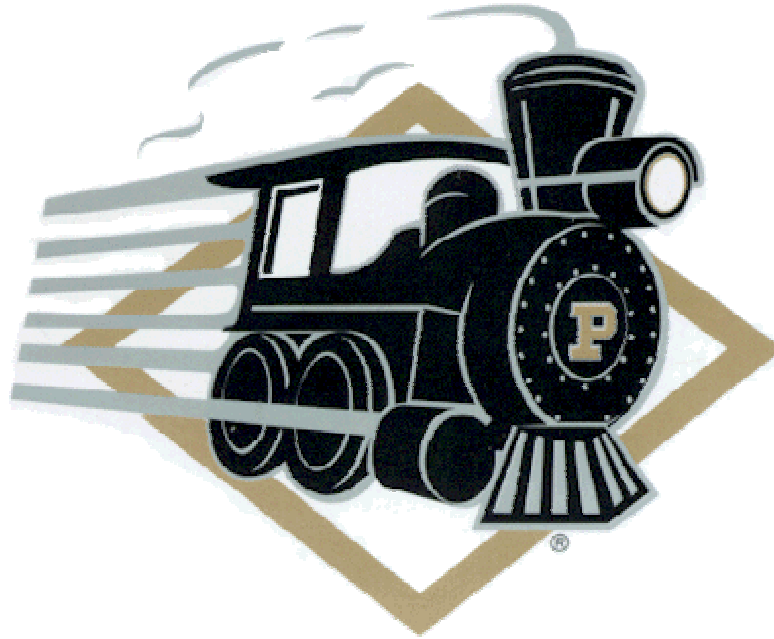


Verification of the quasi-steady approximation for sound generation by confined pulsating jets



L. Mongeau, Z. Zhang, S. Thompson, and S.H. Frankel
School of Mechanical Engineering
Purdue University

The 3rd Biennial ICVPB Meeting
Sept. 13-16 2002, Denver, Colorado

For more information:

see web site at:

<http://widget.ecn.purdue.edu/%7Evoice/>

<http://widget.ecn.purdue.edu/%7Evoice/>



Acknowledgements

Sponsor

- subcontract, NIDCD (R01 DC03577)
- Ronald C. Scherer, P.I., BGSU

Graduate Students

- Zhaoyan Zhang (Postdoc, U. Maryland)
- Scott Thomson (Ph.D., summer 2003)
- Jong Beom Park

Collaborators

- Steve H. Frankel, Assoc. Prof.

Technical Assistance

- Gilbert Gordon



Objectives

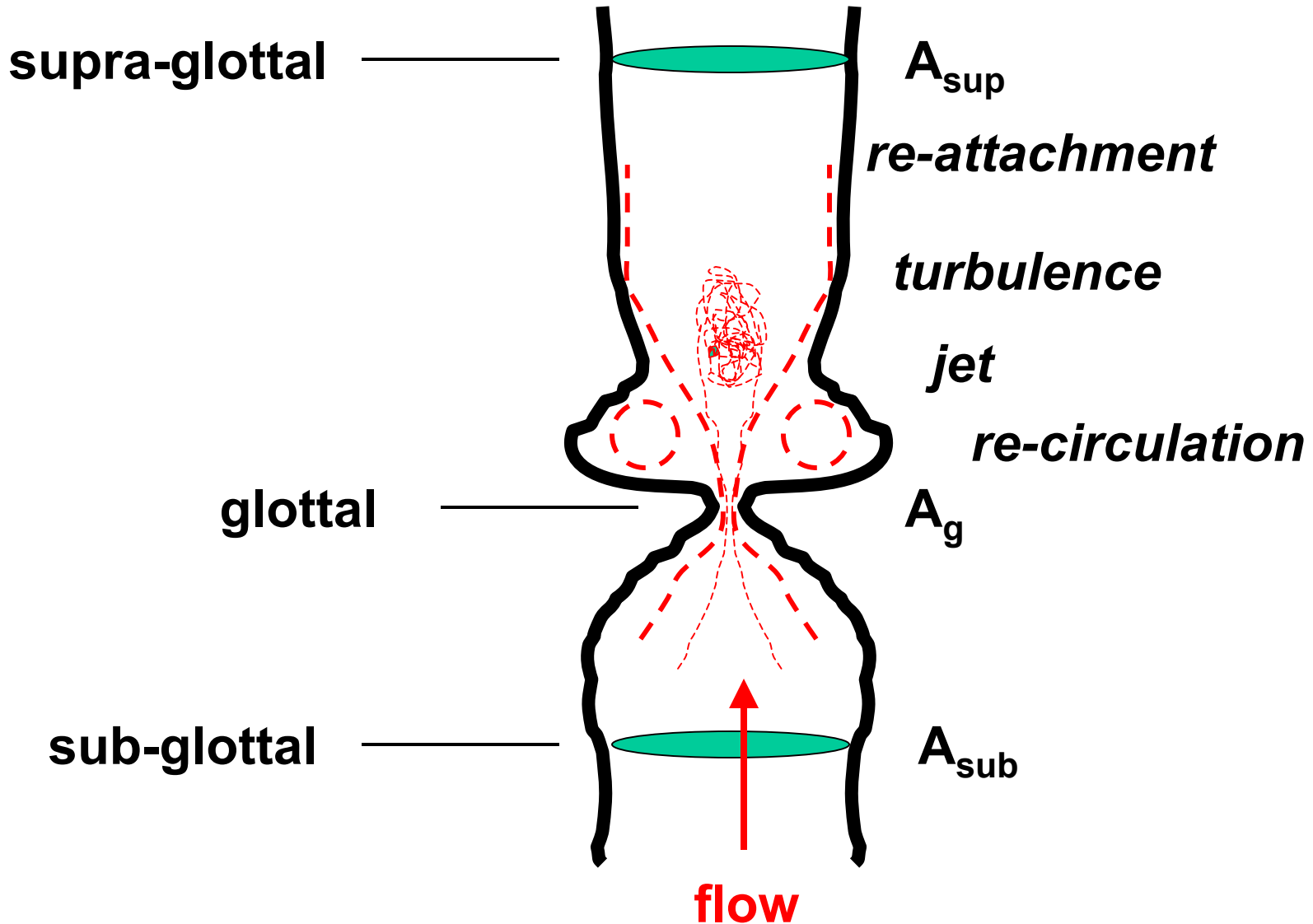
Investigate the range of validity of the quasi-steady approximation

- Periodic Component
- Random, broadband component

Gain a better understanding of the sound generation mechanisms

- periodic and broadband components
- steady and pulsating confined jet flows

Intra-Glottal Flows



The 3rd Biennial ICVPB Meeting
Sept. 13-16 2002, Denver, Colorado

Bernoulli's equation

$$p_{\text{sub}} - p_{\text{sup}} = \frac{1}{2} \rho_0 U_c^2$$

assumptions:

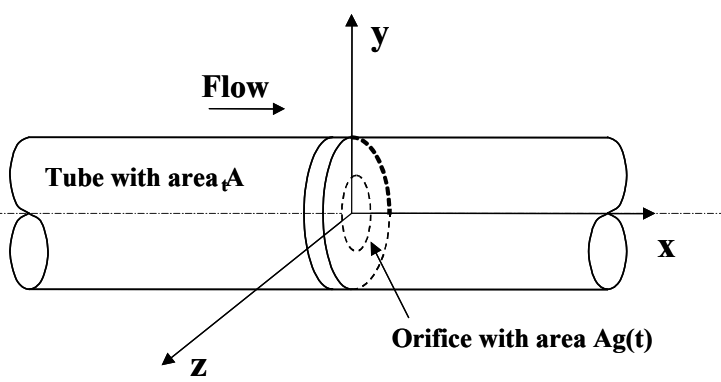
- irrotational
- flow incompressible
- along a streamline
- viscous effects neglected
- acceleration effects neglected

Bernoulli's Obstruction Theory

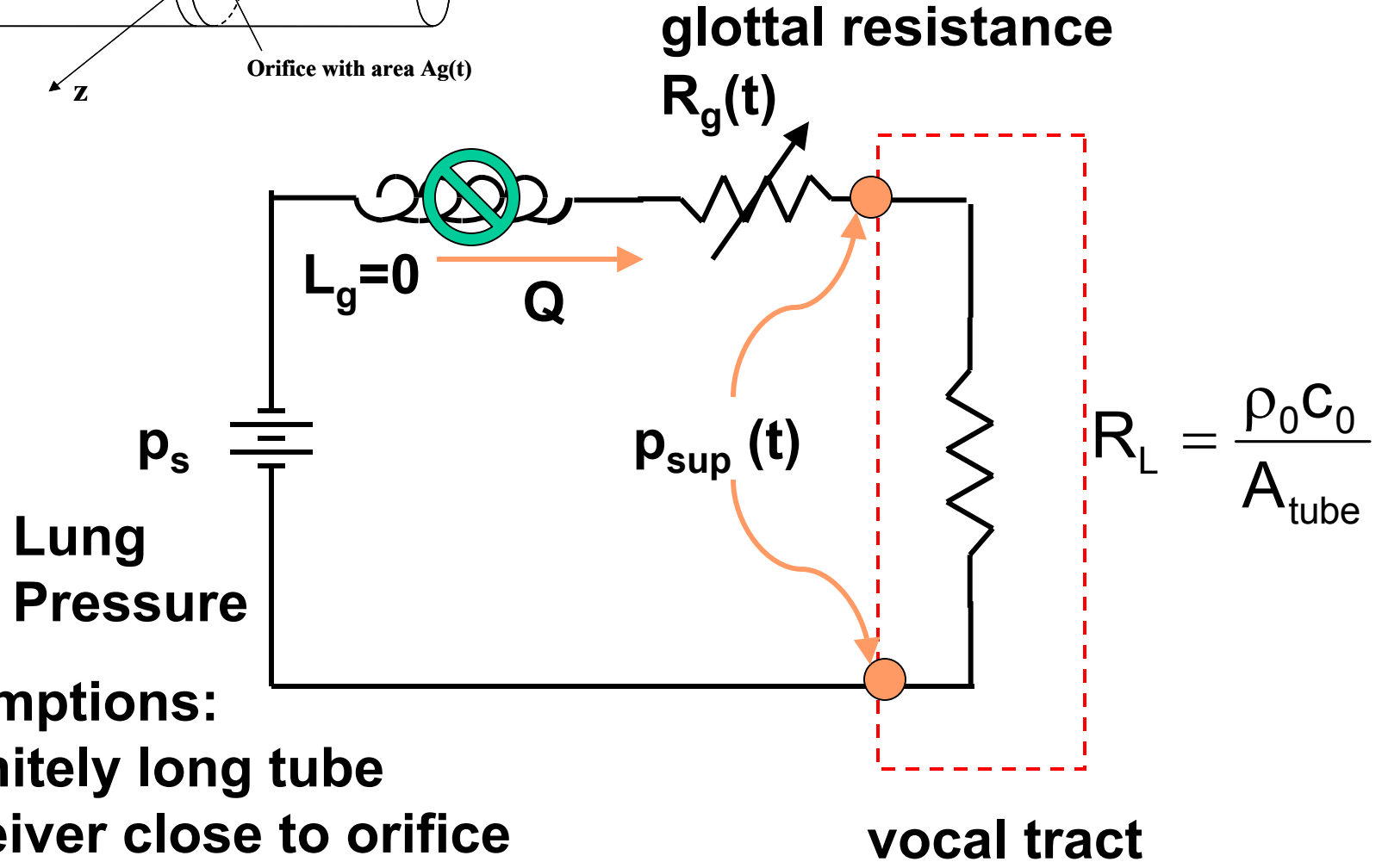
$$Q = KA_g \sqrt{\frac{2(p_{\text{sub}} - p_{\text{up}})}{\rho_0}}$$

assumptions:

- large area ratio A_{sub}/A_g
- flow coefficient K combines discharge coefficient and approach velocity factor
- $K=K(\text{shape, area, inflow+outflow condition})$
- same as Bernoulli's equation
- all variable instantaneous (except density)



Simplified Circuit



assumptions:

- infinitely long tube
- receiver close to orifice
- negligible inductive effects

Glottal Resistance

$$R_g = \frac{p_{\text{sub}} - p_{\text{up}}}{Q} = \frac{p_{\text{sub}} - p_{\text{up}}}{KA_g \sqrt{\frac{2(p_{\text{sub}} - p_{\text{up}})}{\rho_0}}}$$

- $K=K(A_g, p_{\text{sub}} - p_{\text{sup}})$
- direct measurement of A_g , p_{sup} , p_{sub} sufficient to calculate R_g
- *quasi-steady approximation states that for given geometry, A_g and Δp , R_g is the same for steady or pulsating flows*

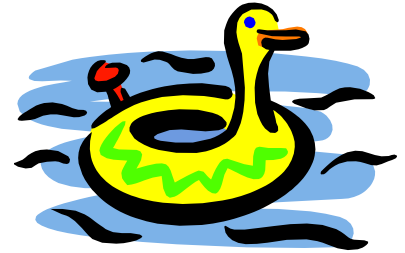
Non-Stationary Phenomena

- $d\phi/dt$
- **Vorticity shedding**
- **Large scale turbulent structures**
- **Flow induced by motion of wall**

Rubber Dynamic Physical Models

Advantages

- real size (no need for scaling)
- allow acoustic and simple flow measurements
- orifice shape easy to modify
- easy to add complexity to model geometry



Disadvantages

- real size (can't easily perform detailed flow measurements for validation of CFD)
- some shape distortion at high frequency



Experimental Facility

Inertial base (concrete slab)

Two large electro-dynamic shakers+power amplifiers

Rectangular Acrylic test sections

- anechoic terminations
- open tubes of different lengths

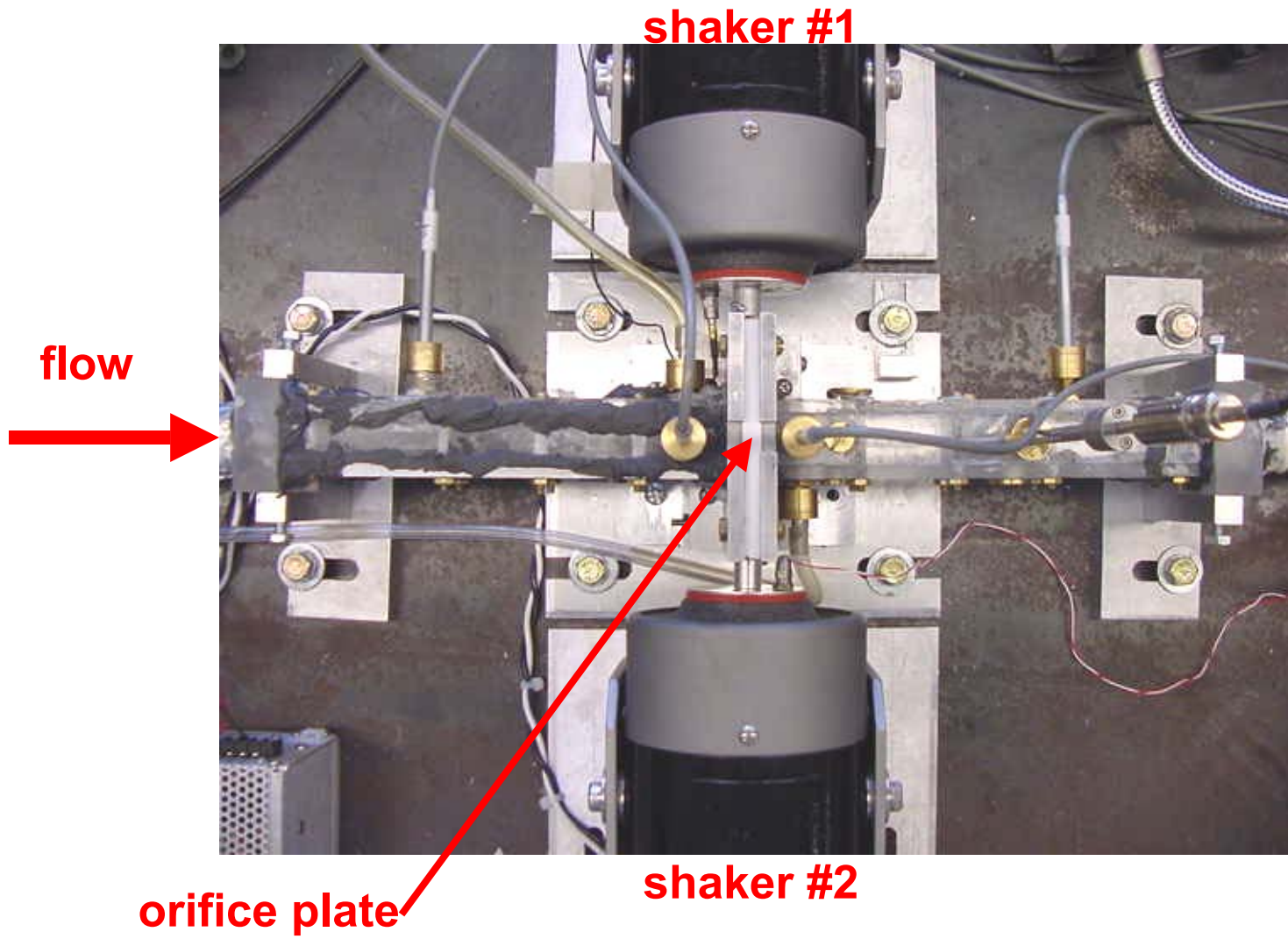
Flow supply and controller

- air, helium, and CO₂ mixtures

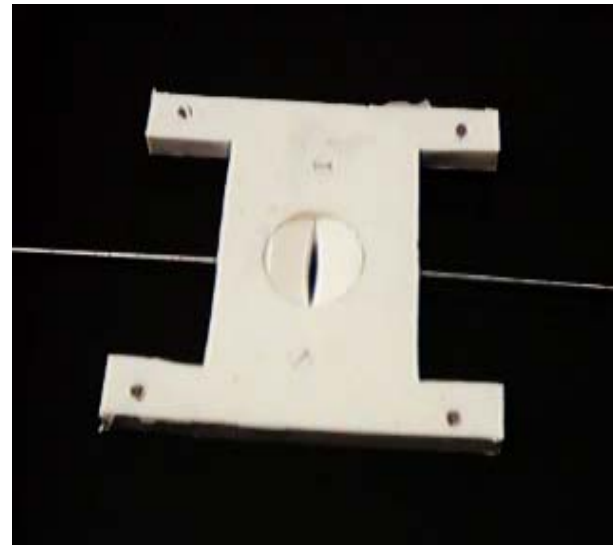
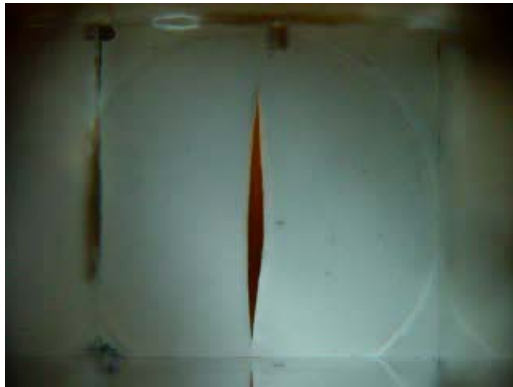
Rubber glottis models (real size)

- molds machined using Stereo Lithography
- geometry defined using CAD (proE)
- three geometries (convergent, straight, and divergent)

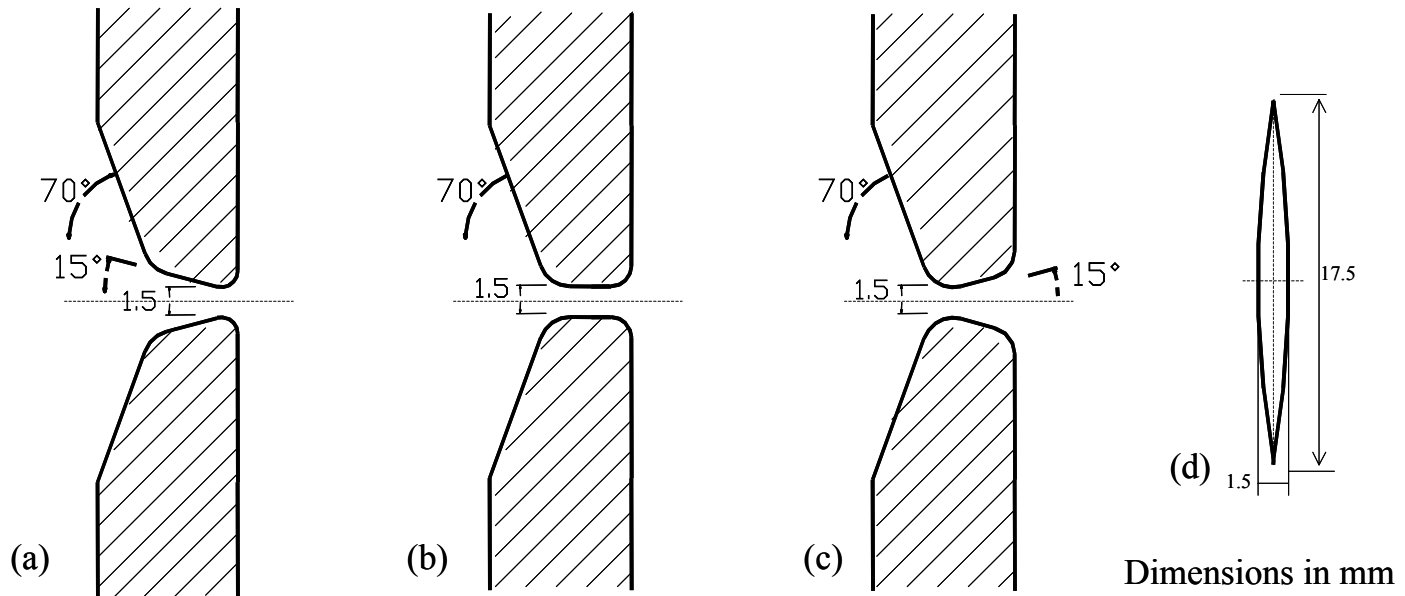
Belt mechanical drive used for flow visualization



The 3rd Biennial ICVPB Meeting
Sept. 13-16 2002, Denver, Colorado

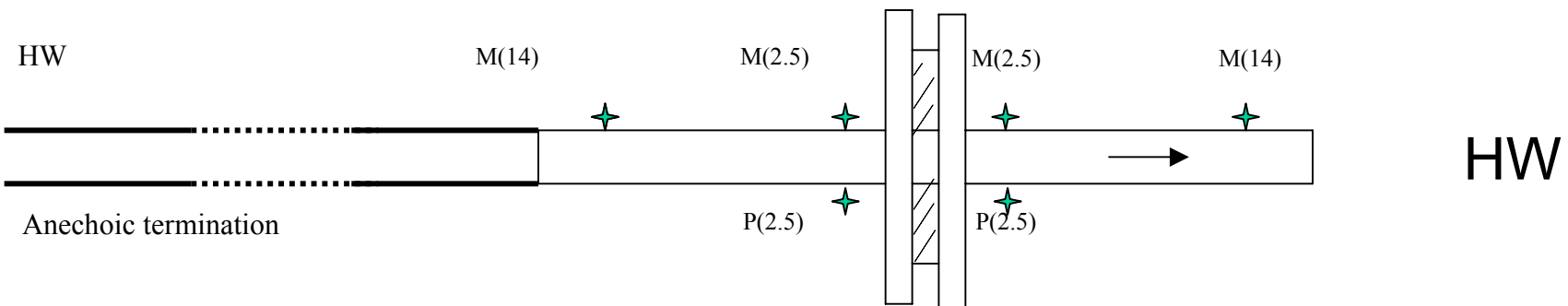
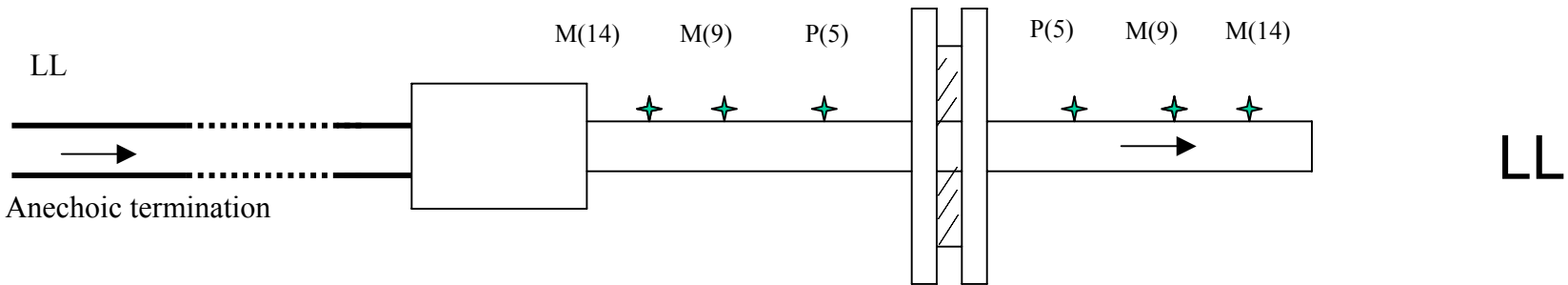
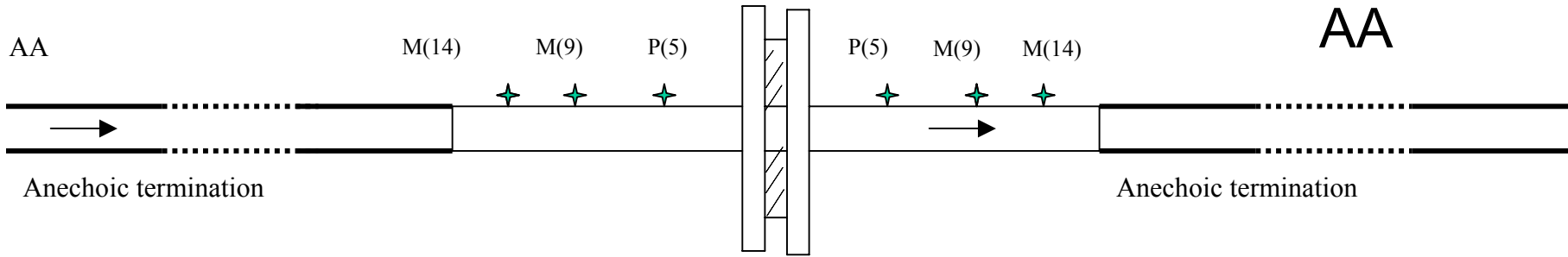


100 Hz

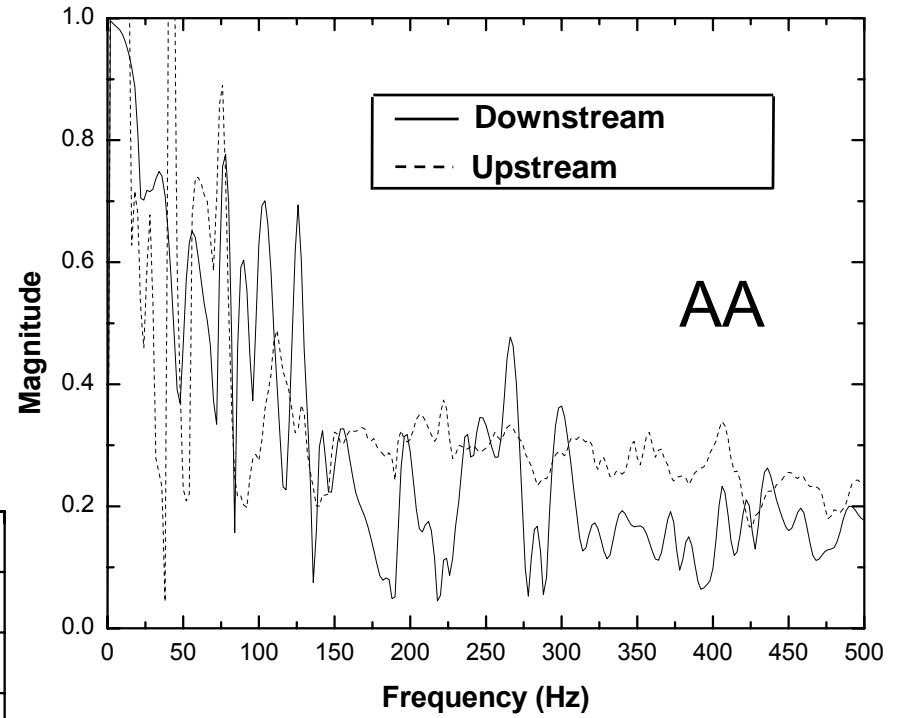
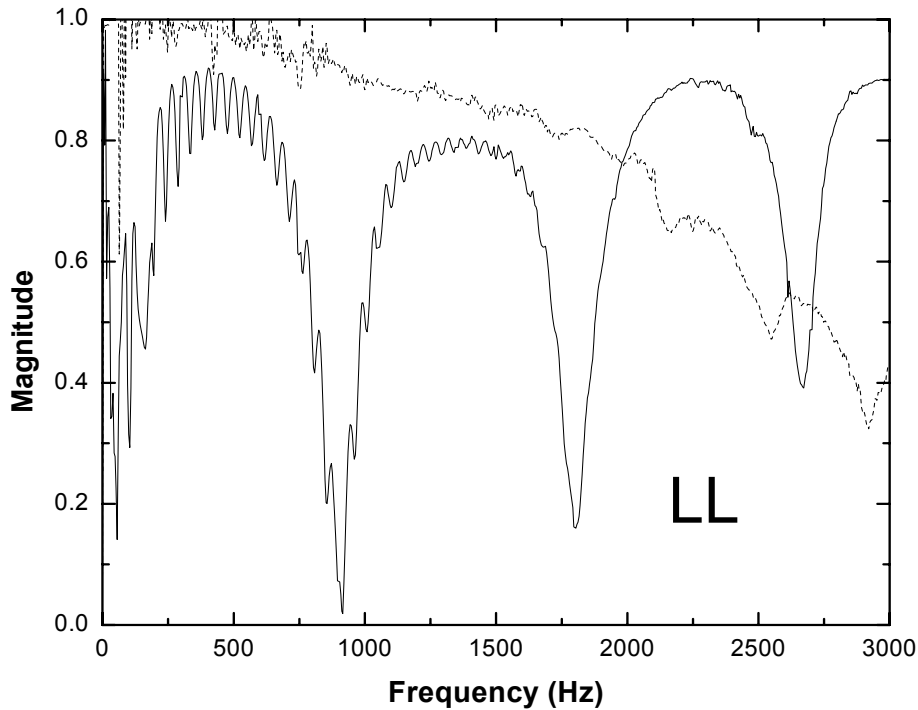


The 3rd Biennial ICVPB Meeting
Sept. 13-16 2002, Denver, Colorado

Tube configurations



Reflection coefficients



Instrumentation

Two pairs of phased-matched microphones

Precision manometer

Precision gas flow meter

Photoelectric detector and light source

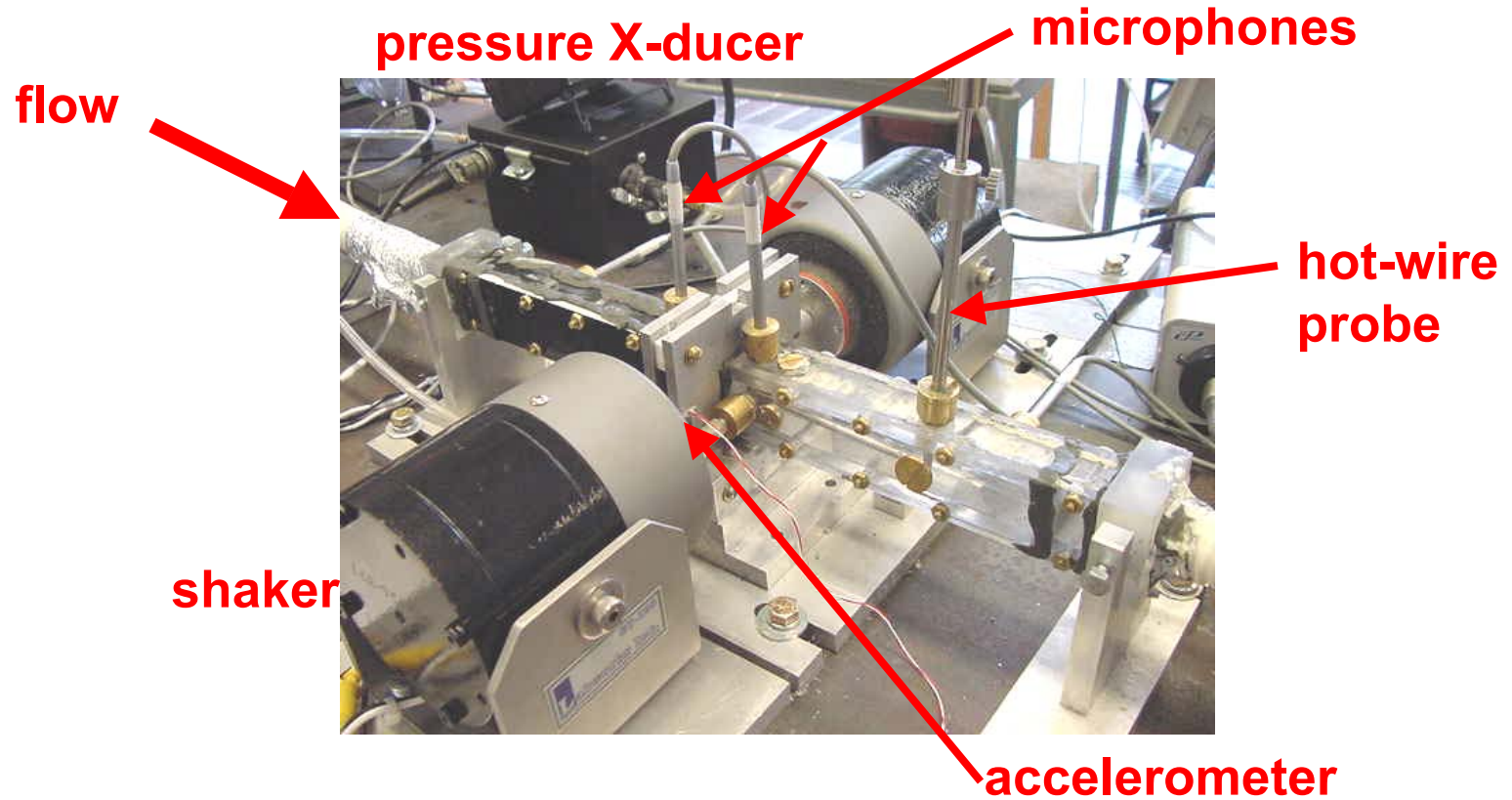
Accelerometers

Hot-wire anemometer (up to 6 channels)

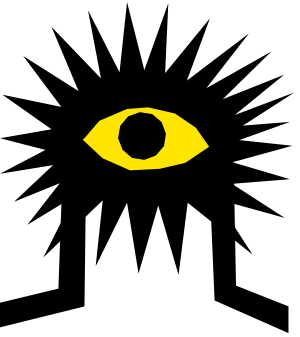
Data acquisition systems

Smoke generator

High-speed camera (NAC)



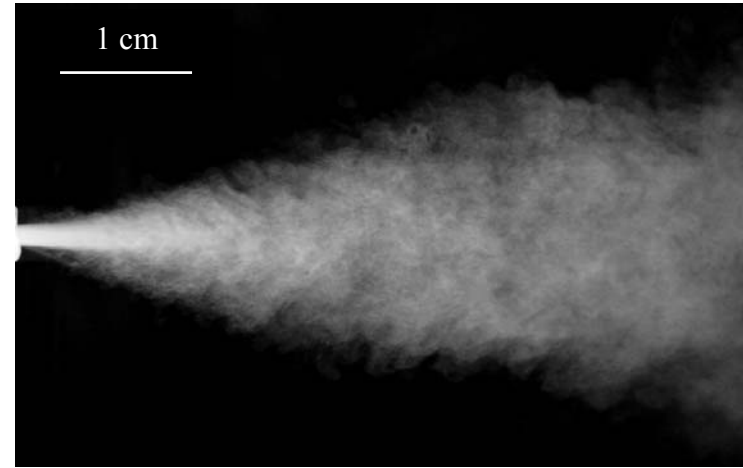
The 3rd Biennial ICVPB Meeting
Sept. 13-16 2002, Denver, Colorado



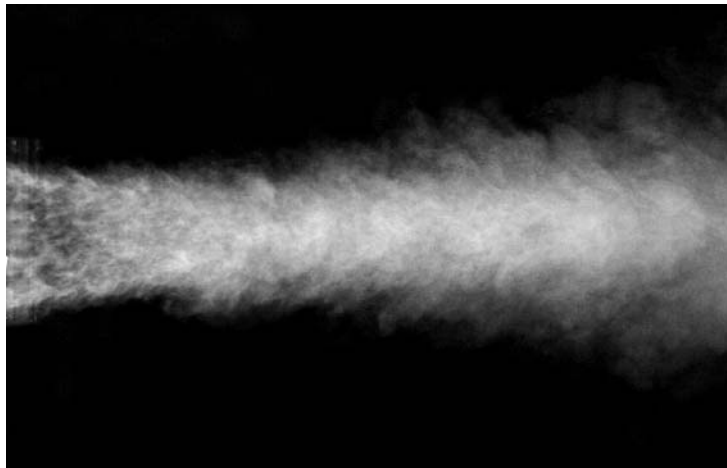
Flow Visualization

steady open jet, 4 cm H₂O

converging



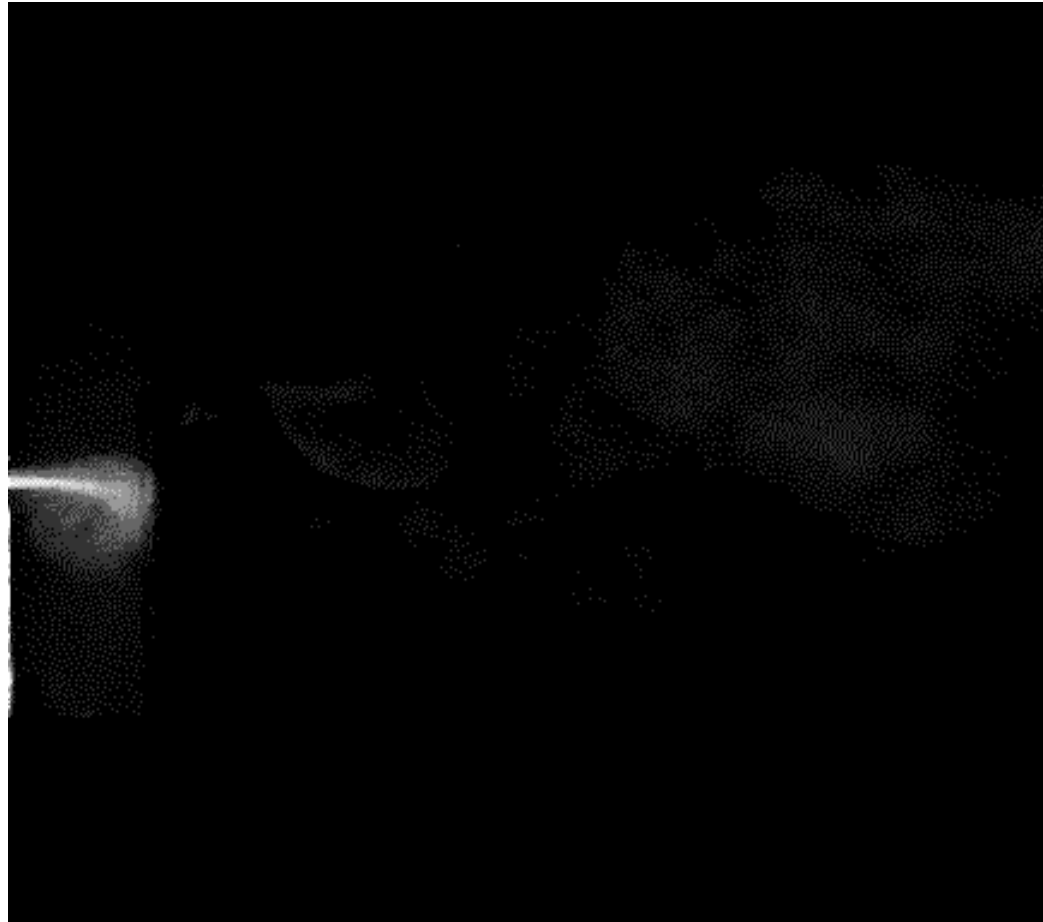
diverging



span view

width view

The 3rd Biennial ICVPB Meeting
Sept. 13-16 2002, Denver, Colorado



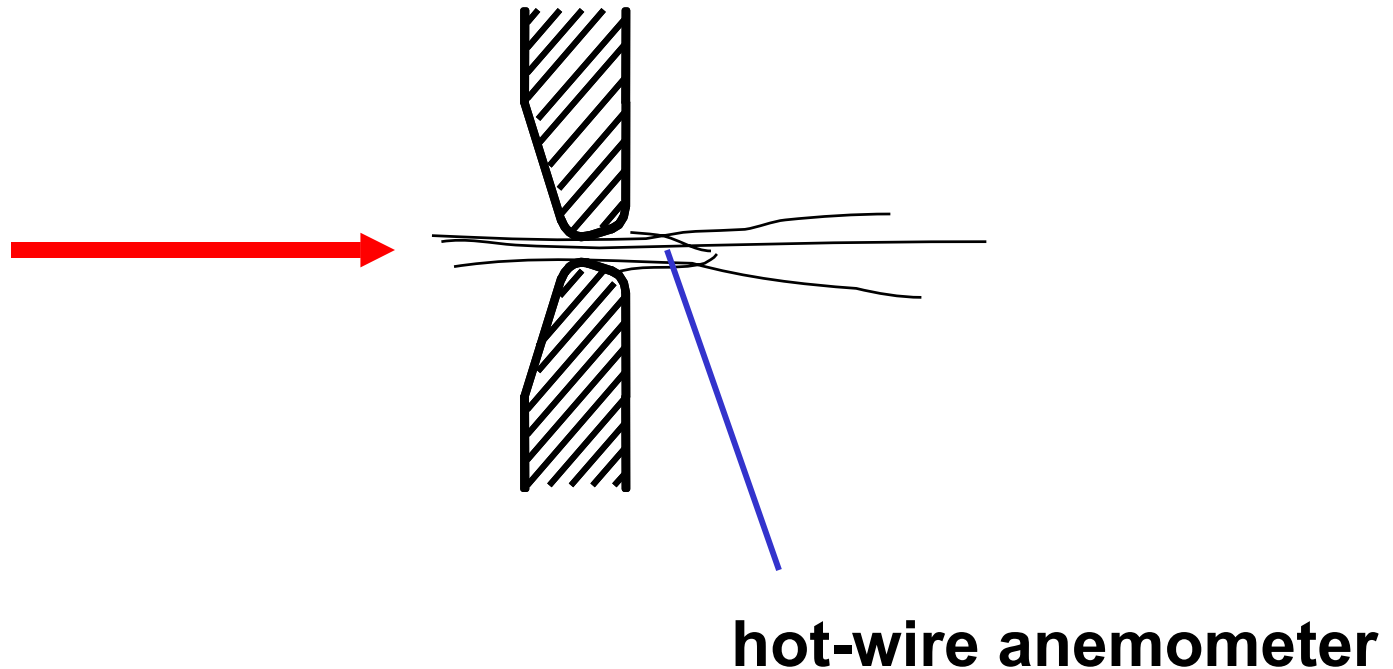
The 3rd Biennial ICVPB Meeting
Sept. 13-16 2002, Denver, Colorado



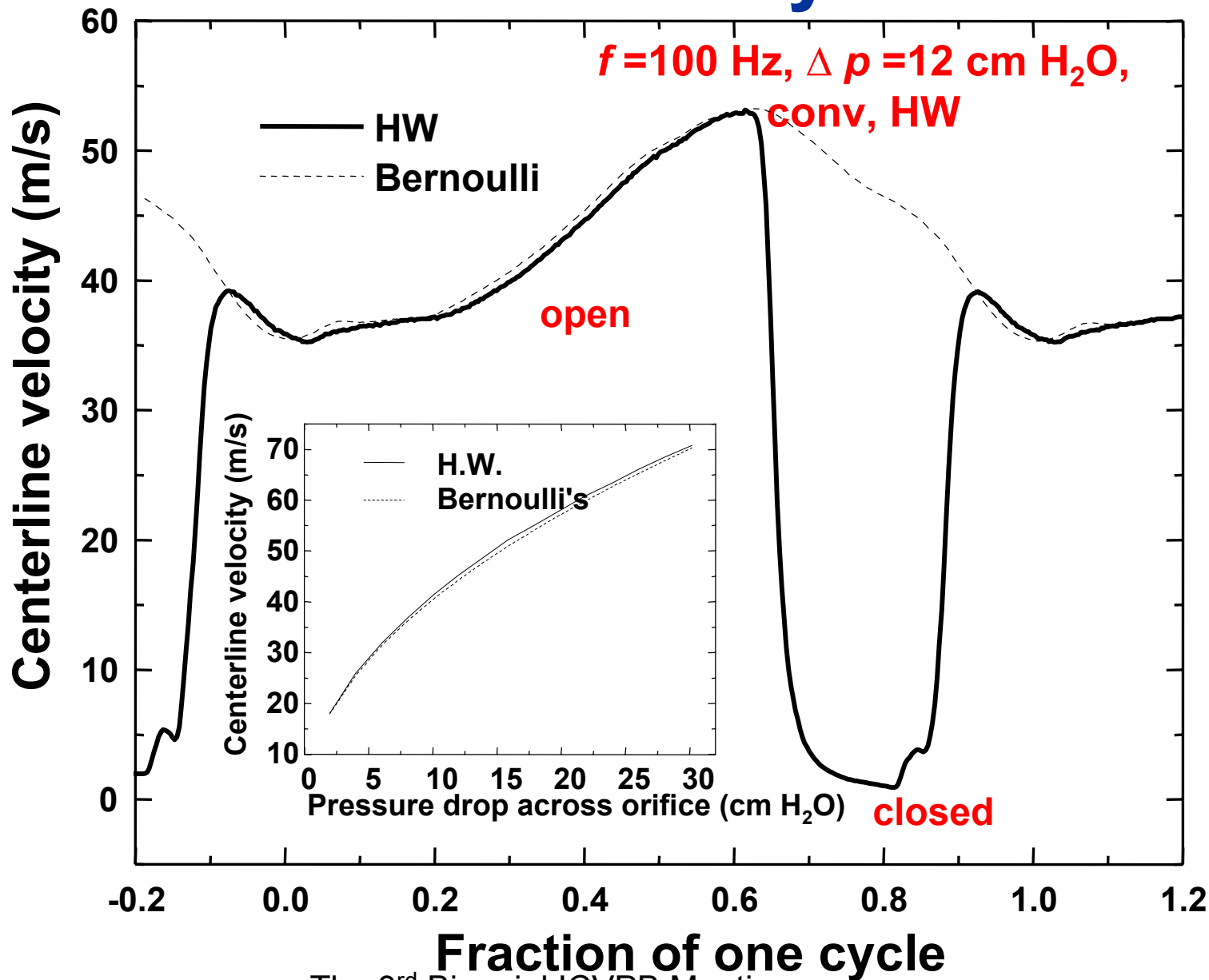
The 3rd Biennial ICVPB Meeting
Sept. 13-16 2002, Denver, Colorado

Bernoulli's Equation

Direct verification



Hot-wire velocity data



Bernoulli's Obstruction Theory

Indirect Method

- can't easily measure instantaneous flow rate
- use inverse filter method
 - equivalent monopole strength

Assumptions

- **flow through orifice at any instant same as steady incompressible flow for same wall geometry and inlet boundary condition**
- **monopole source**
- **plane waves**
- **source strength is fluctuating volume velocity at orifice**

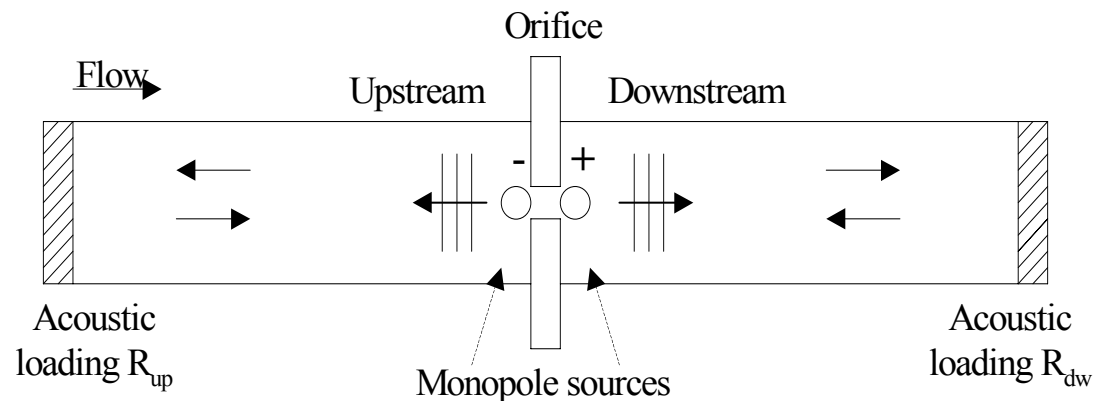
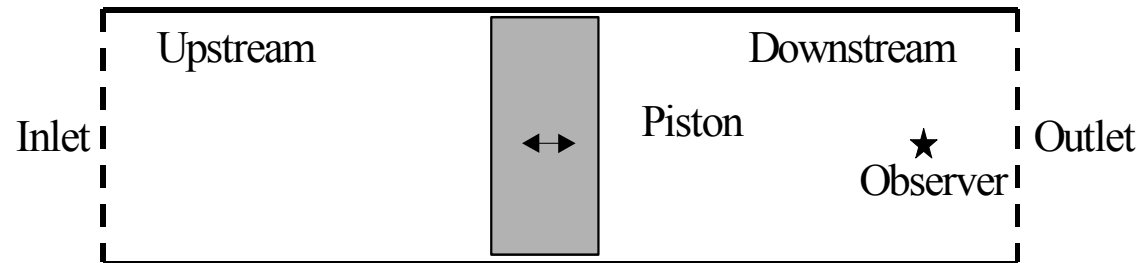
Procedures

- iteration method
- Predict sound pressure using Bernoulli's equation (steady form), using measured orifice area, mean pressure drop across the orifice, and orifice discharge coefficients measured statically
- Reflections accounted for using signal processing techniques (deconvolution)
 - two-microphone method
 - low-pass filter



equivalent monopole source model

- Dipole source due to unsteady pressure drop
- similar to vibrating piston
- Decompose into two monopole sources with equivalent source strength, each radiating to one side of the orifice
- two equivalent monopole sources equal in strength and opposite in phase



$$\Delta p(t) = \Delta p_0 + p'_{up}(0, t) - p'_{dn}(0, t) = \frac{1}{2} \rho_0 U_c^2$$

$$Q = C_d A_g U_c$$

$$u'_{up}(0, t) = \int \frac{B_{up}(0, \omega)}{\rho_0 c} \{e^{j(\omega t - kL)} - R \cdot e^{j(\omega t + kL)}\} d\omega = -\frac{1}{A_t} \{Q(t) - Q_0\}$$

$$u'_{dn}(0, t) = \int \frac{B_{dn}(0, \omega)}{\rho_0 c} \{e^{j(\omega t - kL)} - R \cdot e^{j(\omega t + kL)}\} d\omega = \frac{1}{A_t} \{Q(t) - Q_0\}$$

$$p'(x, t) = \int B(x, \omega) \{e^{j(\omega t - k(L-x))} + \hat{R} \cdot e^{j(\omega t + k(L-x))}\} d\omega$$

C_d : orifice discharge coefficient obtained in steady flow measurement

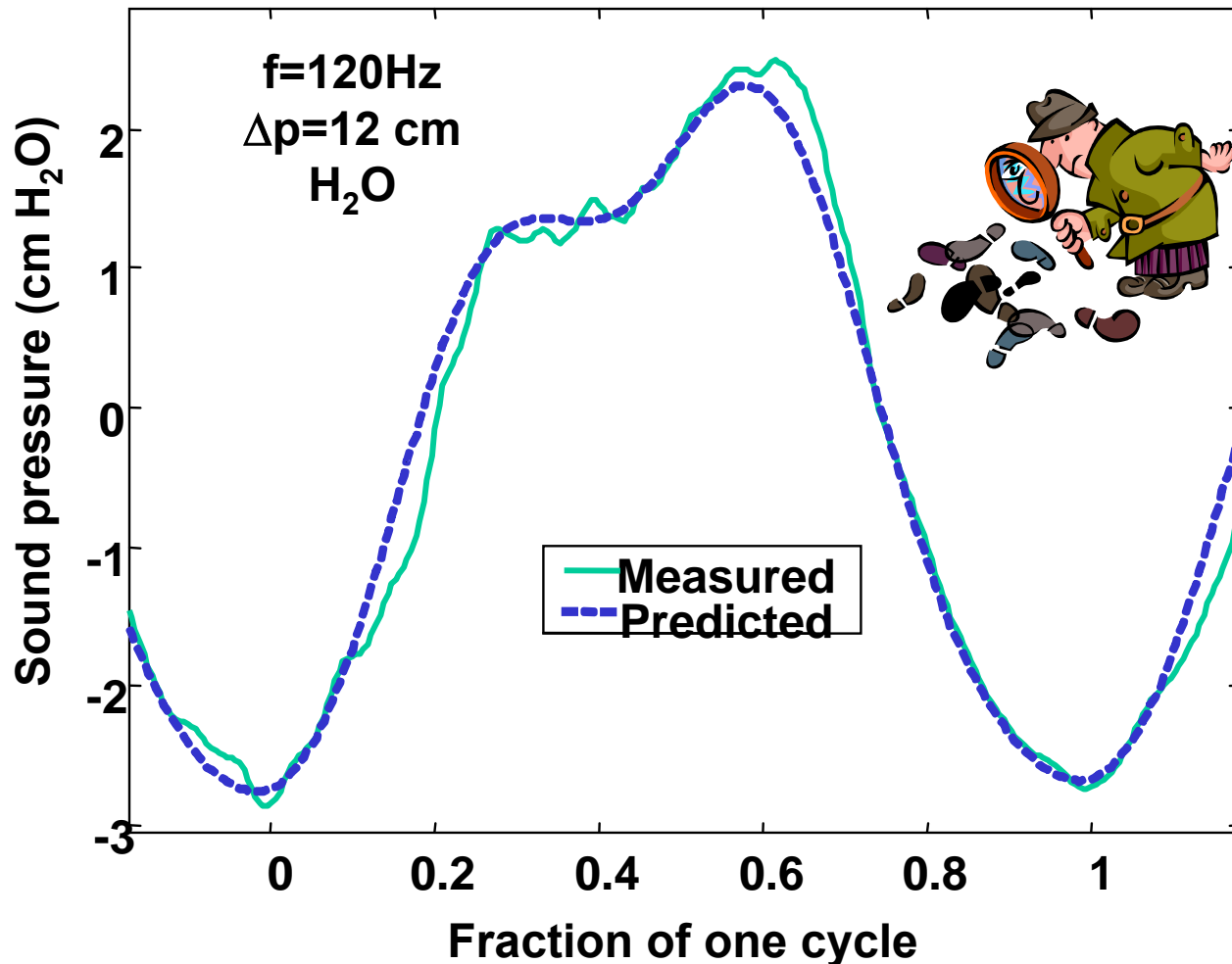
R : reflection factor measured using two-microphone method

B : coefficient to be determined

A_t : orifice area measured using a photoelectric sensor

Typical Result

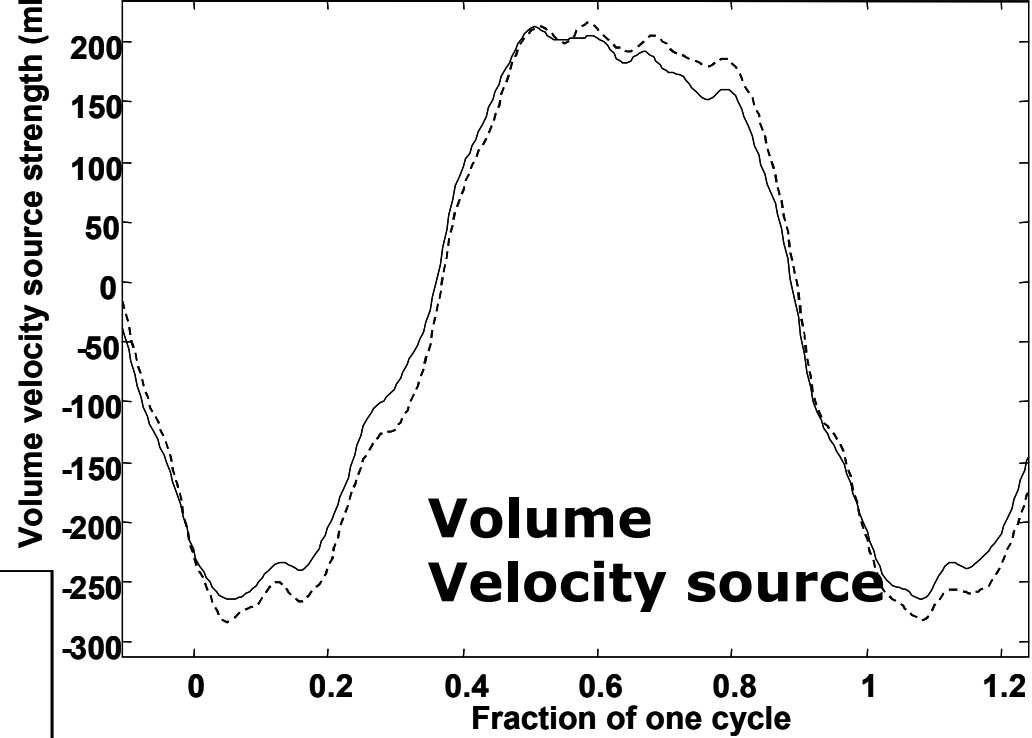
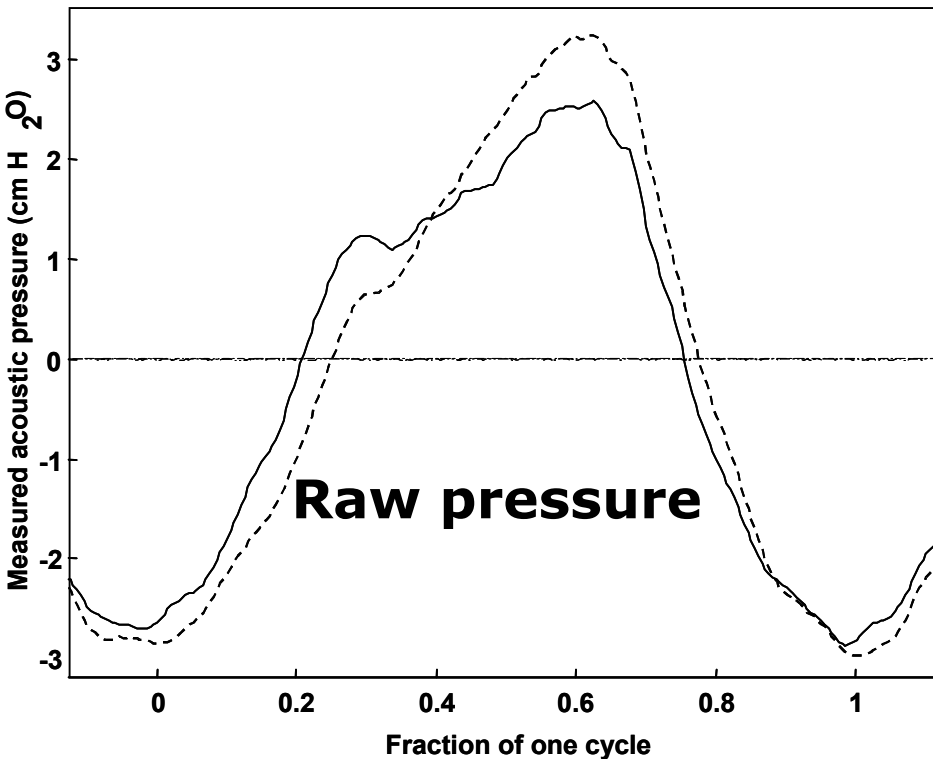
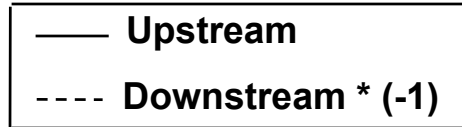
Comparison between measured upstream sound pressure and prediction from quasi-steady assumption



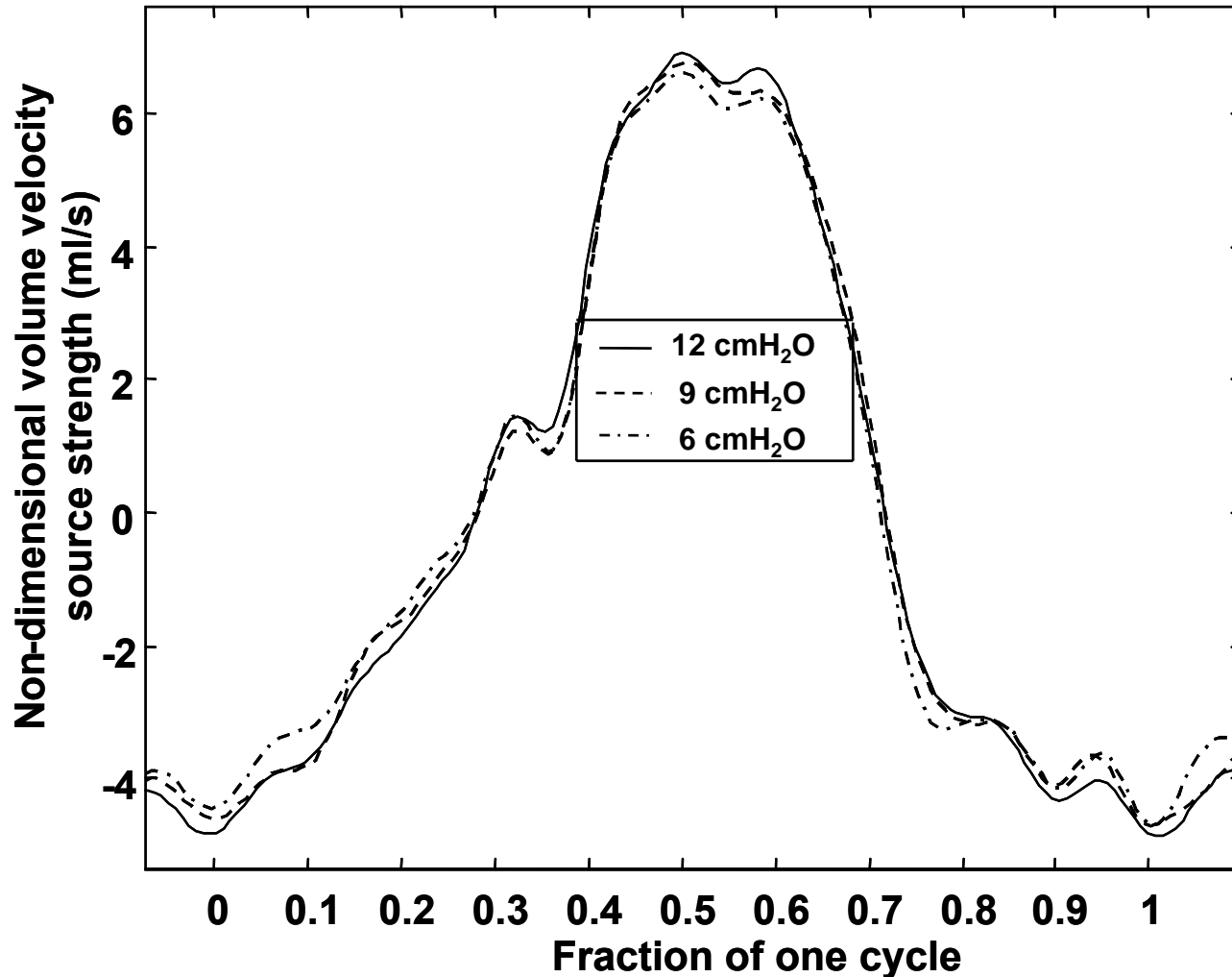
The 3rd Biennial ICVPB Meeting
Sept. 13-16 2002, Denver, Colorado

Results

• $f=80$ Hz, $\Delta p_0=12$ cm H₂O,
convergent orifice, AA

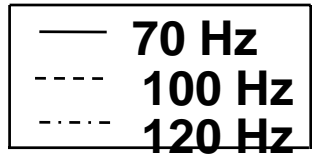


Effects of Mean Pressure

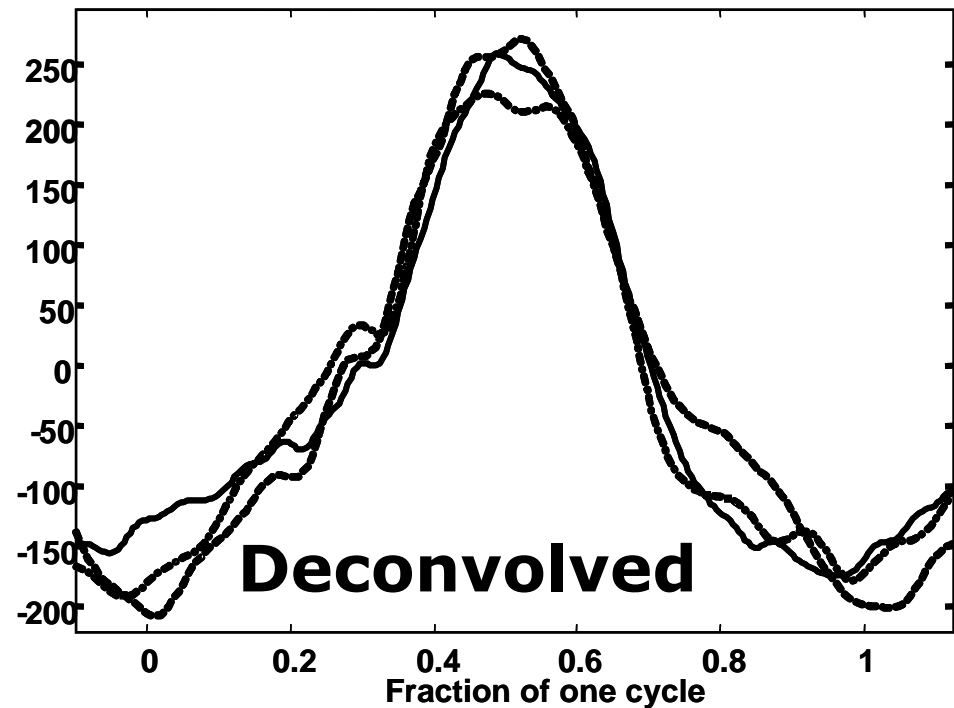
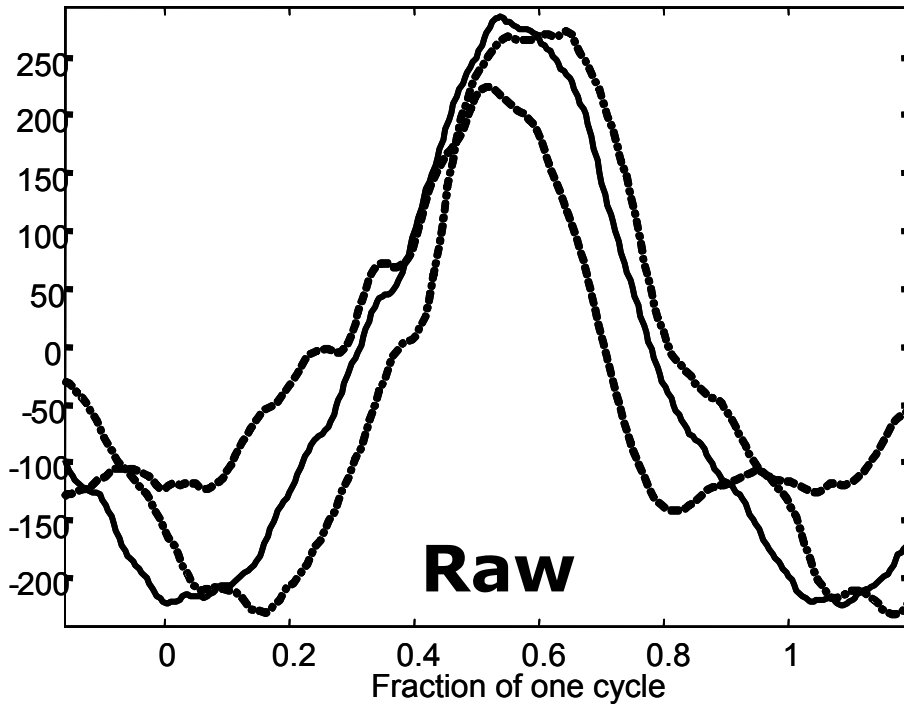


Volume velocity source at different pressure drop scaled by the square root of the mean pressure drop. Straight orifice, $f=120$ Hz.

Effects of Driving Frequency



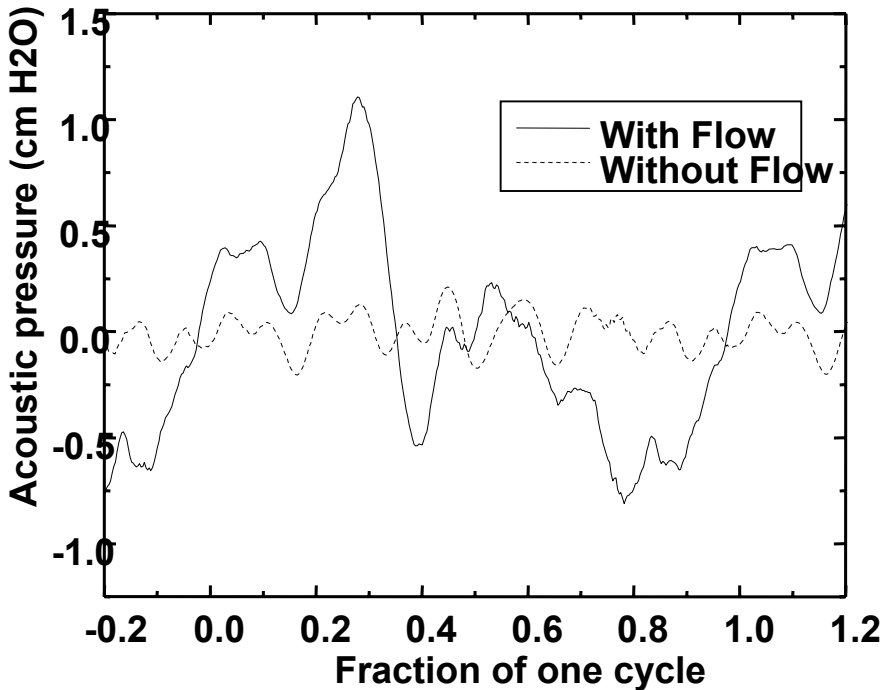
Convergent orifice
 $\Delta p_0 = 12 \text{ cm H}_2\text{O}$



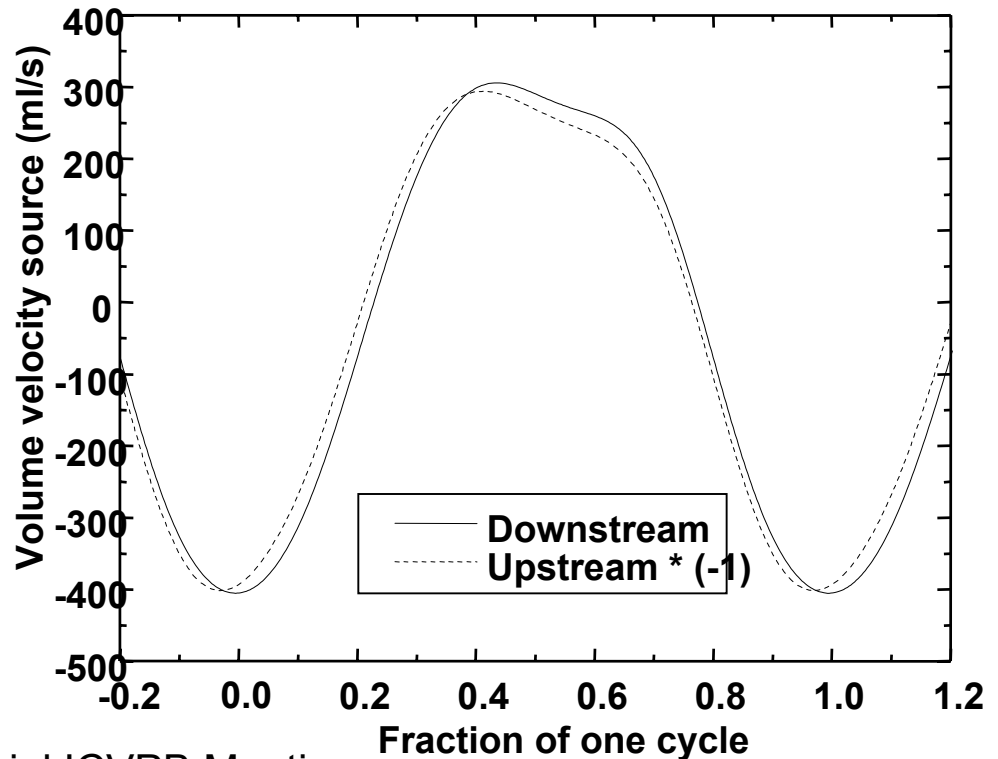
Volume velocity
source strength (ml/s)

- **Driving frequency has small effect on source strength**
- **consistent with quasi-steady assumption**

Effects of acoustic loading



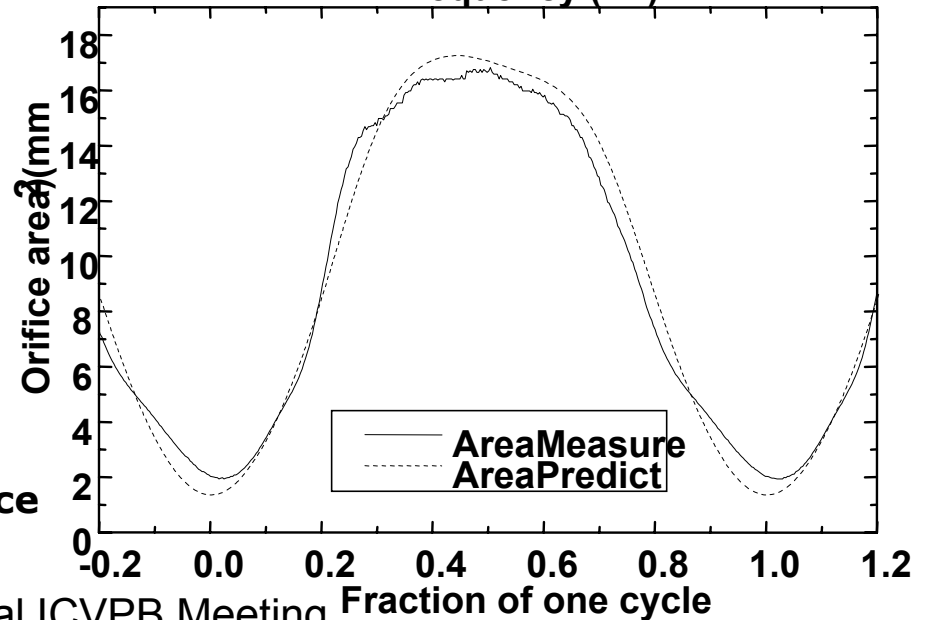
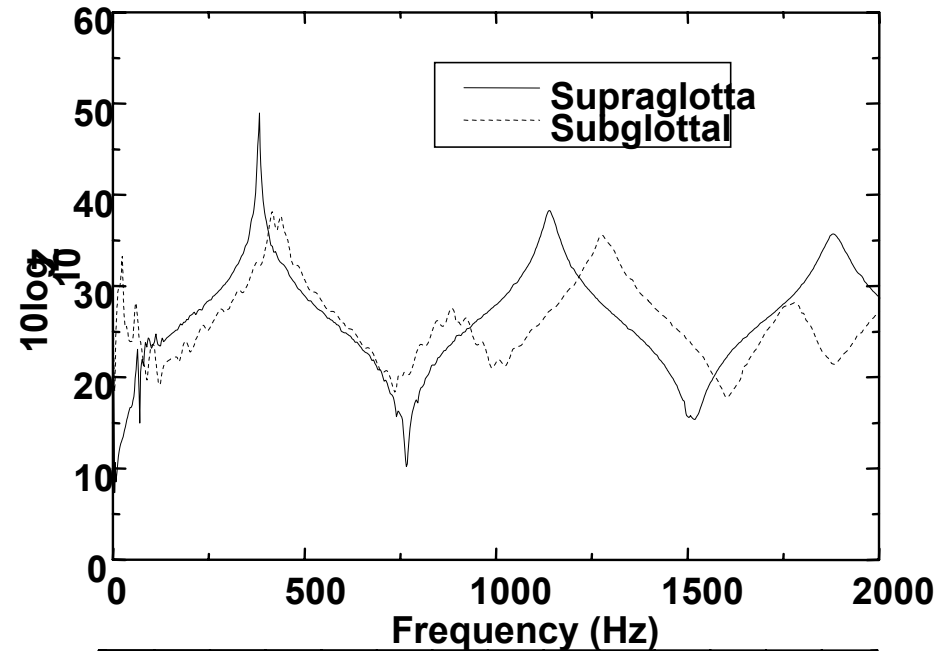
- downstream tube modeled as close-open tube
- velocity node at orifice
- resonance
- monopole ideal velocity source
- monopole source amplified
- dipole source at pressure anti-node



- $f=100$ Hz, $\Delta p_0=12$ cm H₂O, divergent orifice
- Upstream and downstream volume velocity sources agree well

Orifice area function

- Resonance in both subglottal and supraglottal systems (first resonance around 450 Hz)
- This causes errors in reflection coefficient measurements and leads to the failure of the iteration method
- Area can still be predicted using measured sound pressure and statically measured orifice discharge coefficient



$f=100$ Hz, $\Delta p_0=12$ cm H₂O, divergent orifice

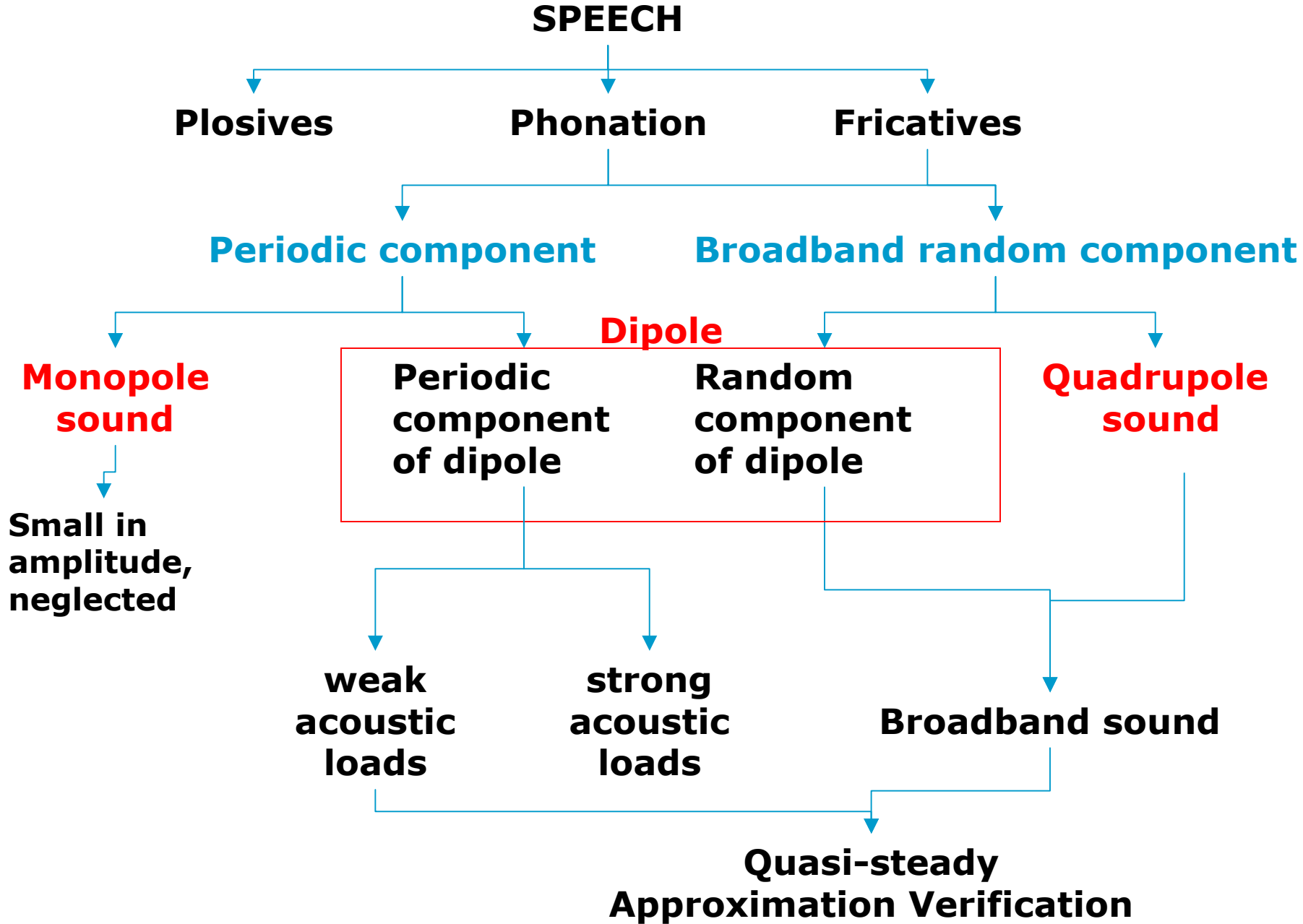
Tonal Component Results

- **Good agreement between measured upstream sound pressure and prediction from quasi-steady assumption**
- **Quasi-steady assumption valid for different orifice shapes at different operating conditions (driving frequency up to 120Hz)**
- **Suggests monopole model could be used in conjunction with 3-D incompressible steady numerical models**

Broadband Sound Production by Non-stationary Turbulent Jets

Periodic component obtained by ensemble-averaging method, and extracted from signals

Statistics of turbulent sound in non-stationary flow at a particular instant compared to those for comparable stationary flow



Broadband Sound in Pulsating Jets

Orifice area is forced at specific frequency

Sound pressure is decomposed into a periodic component and a broadband component

Periodic component obtained by ensemble-average method

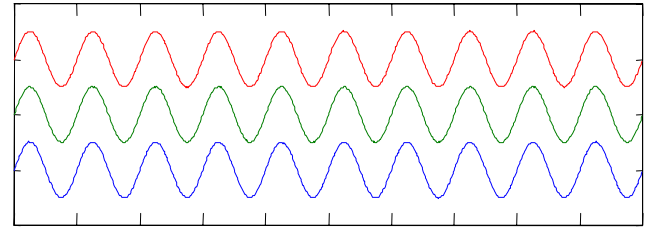
Broadband sound obtained by removing periodic component sound from measured pressure

Characteristics of broadband sound for non-stationary jet at a particular instant compared to those of stationary jets with same flow and orifice geometry

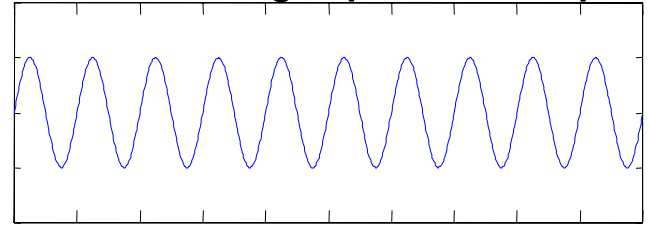
Two methods:

- Probability density function (PDF)
- Wavelet transform

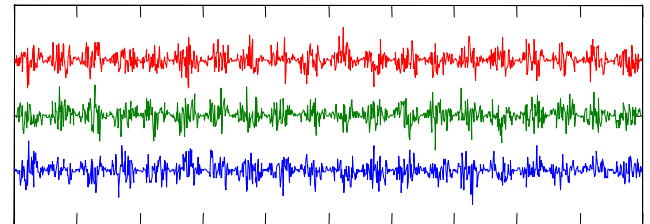
Measured sound pressure



Ensemble-averaged periodic component

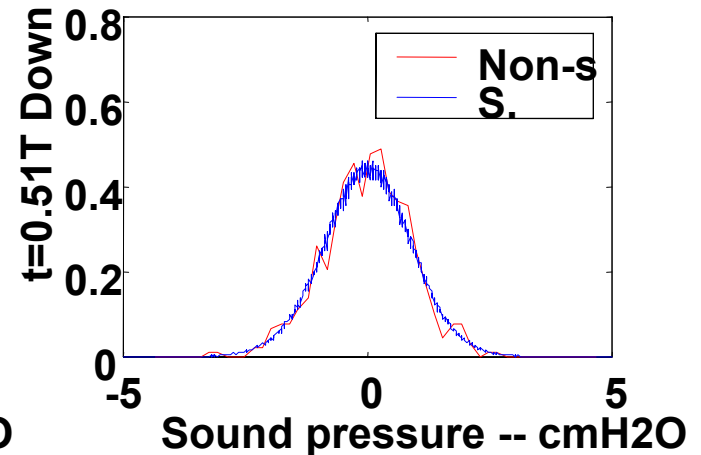
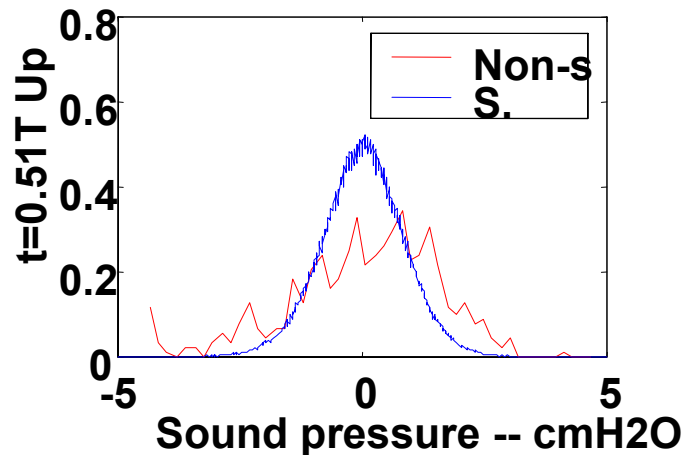
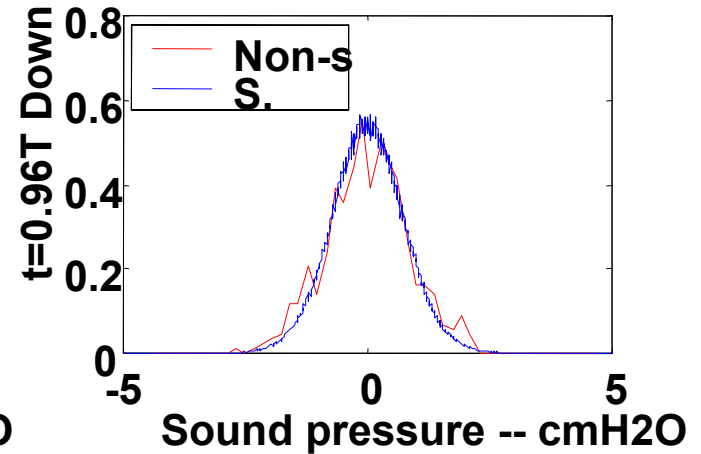
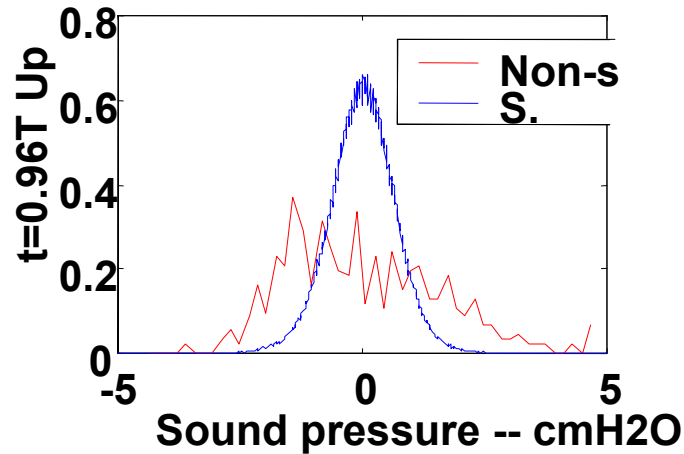


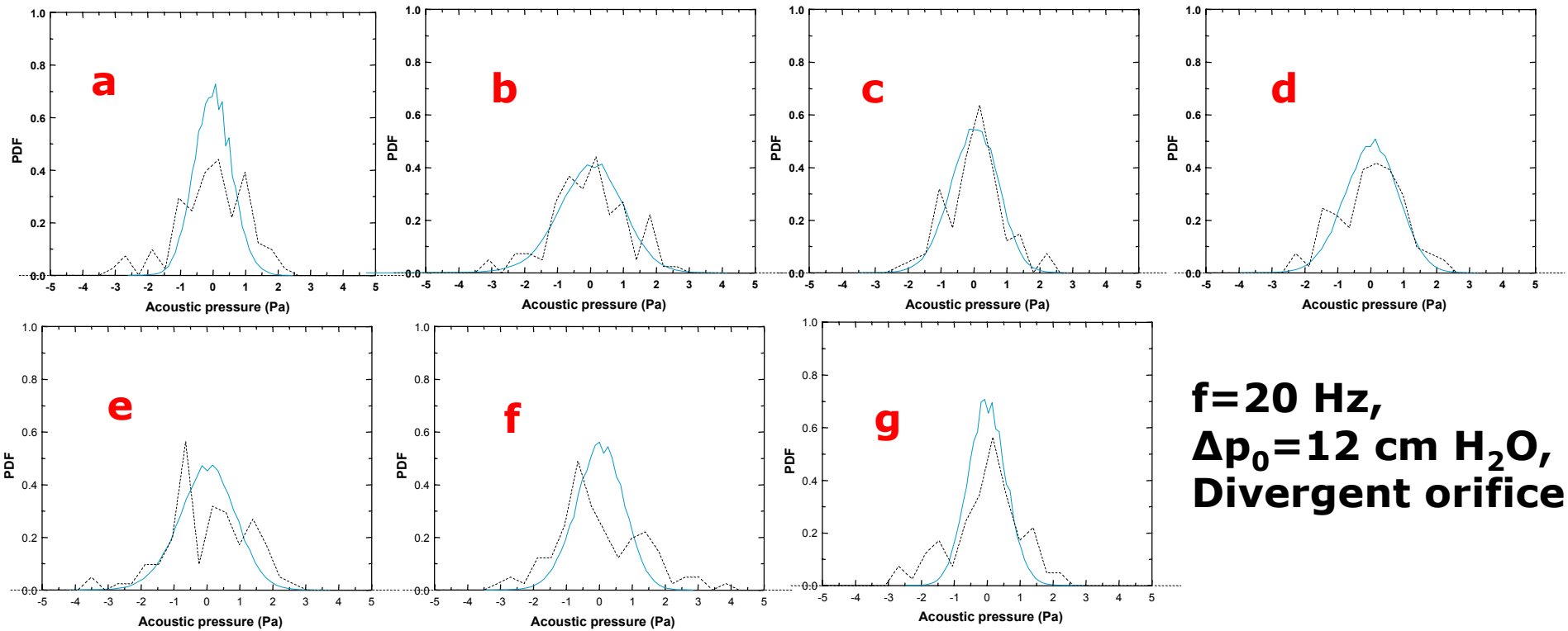
Turbulence generated sound



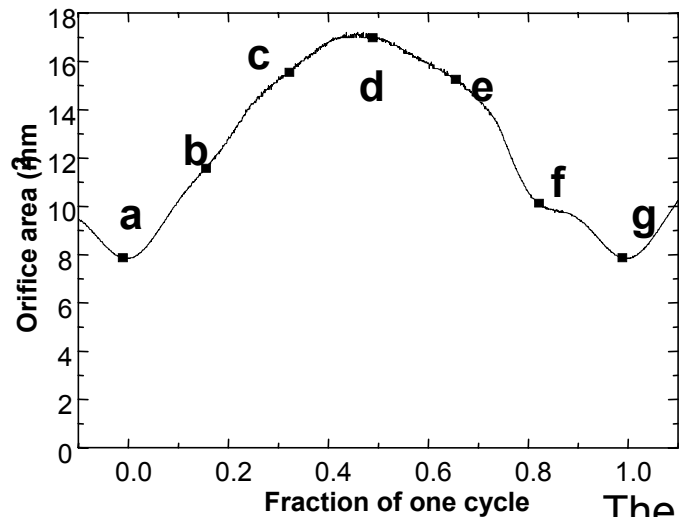
Broadband Sound Production by Non-stationary Turbulent Jets

Comparison between probability density functions

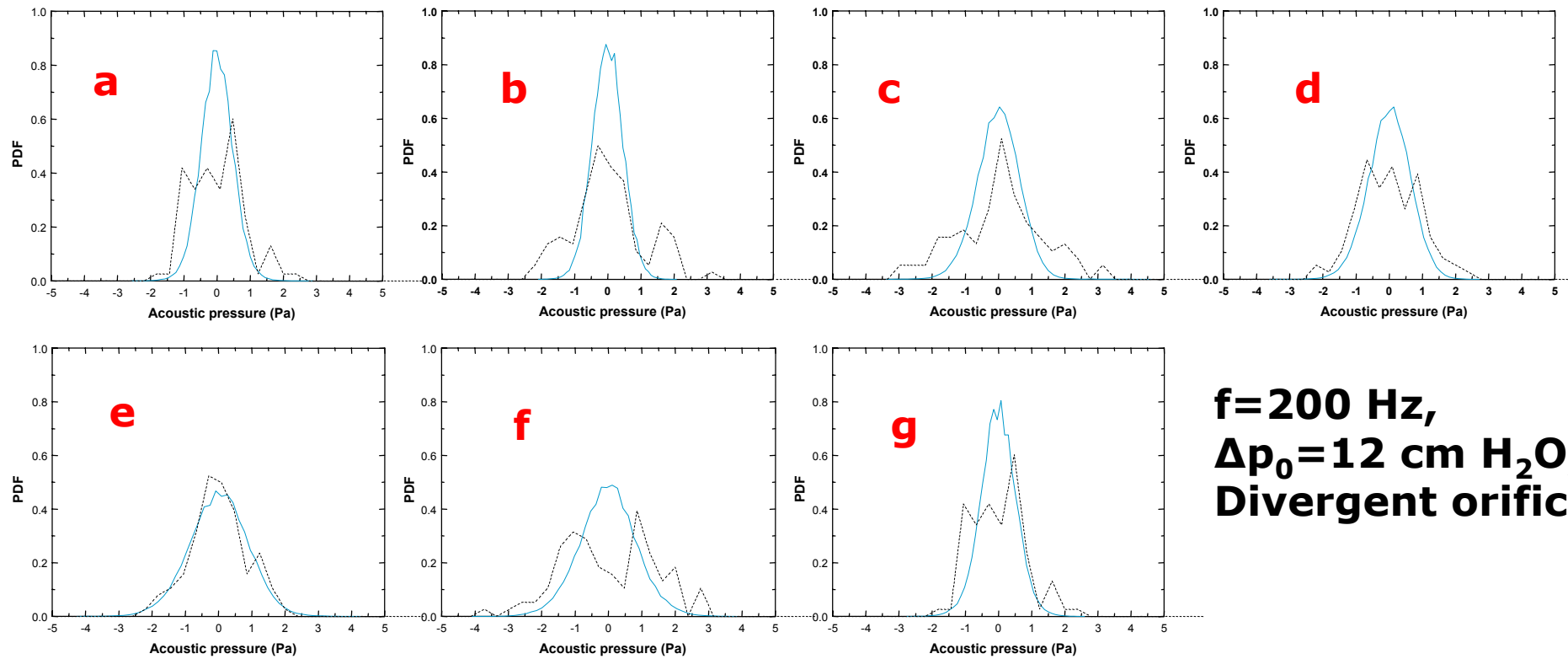




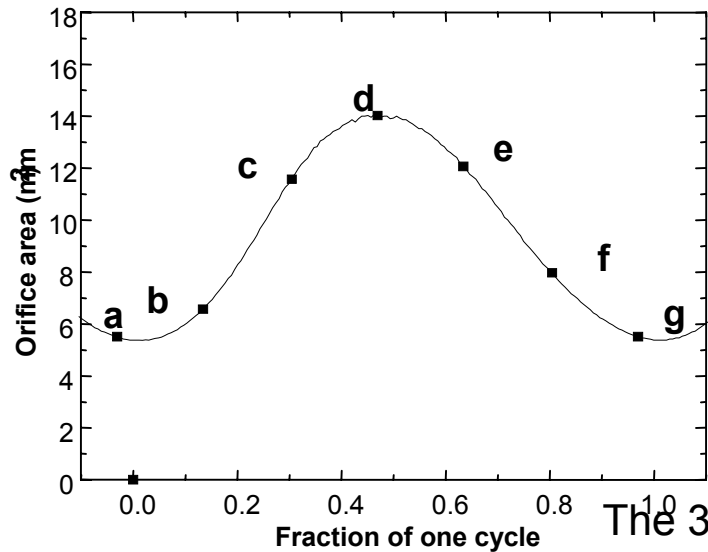
f=20 Hz,
 $\Delta p_0=12$ cm H₂O,
Divergent orifice.



- **Agreement between PDFs evolves during one cycle**
- **Poor agreement during the beginning of orifice opening**
- **Agreement improves as the orifice continues to open**
- **Agreement decreases as the orifice begins to close**



**f=200 Hz,
 $\Delta p_0=12$ cm H₂O,
 Divergent orifice**

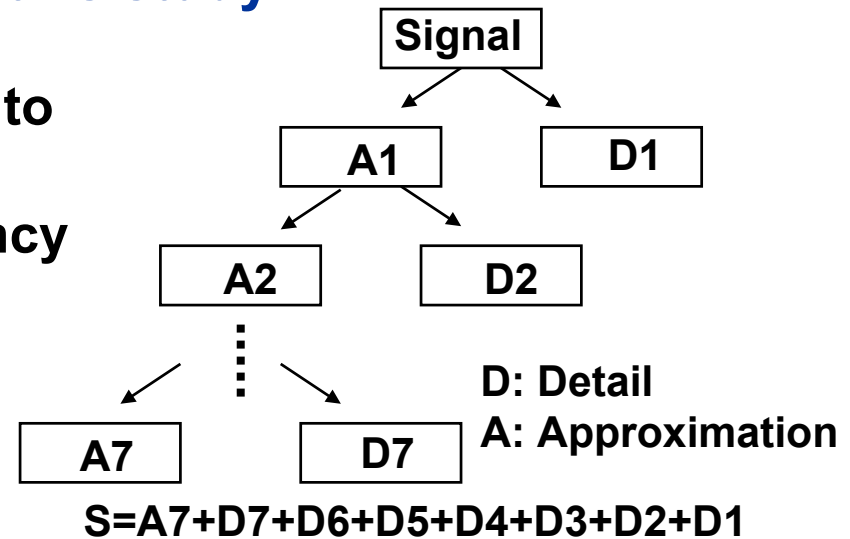


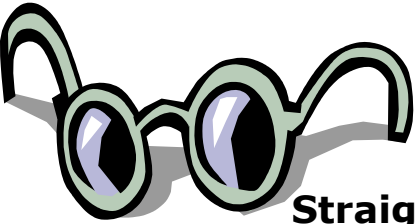
- **As driving frequency increases, general agreement between PDFs decreases, especially during the orifice opening stage**
- **quasi-steady approximation may not be valid for broadband component**

Wavelet Analysis

Provides time information as well as frequency information
In STFT the size of the sliding window is fixed, while in wavelet analysis the window size is changeable, therefore giving same resolution for different frequency component
Daubechies 1 wavelet (a step function) used (similar results obtained with db2)
7-level wavelet transform used in this study

At each level, signal is decomposed into a *Detail* and an *Approximation*. The *Detail* corresponds to the high frequency component while the *Approximation* corresponds to the low frequency component.





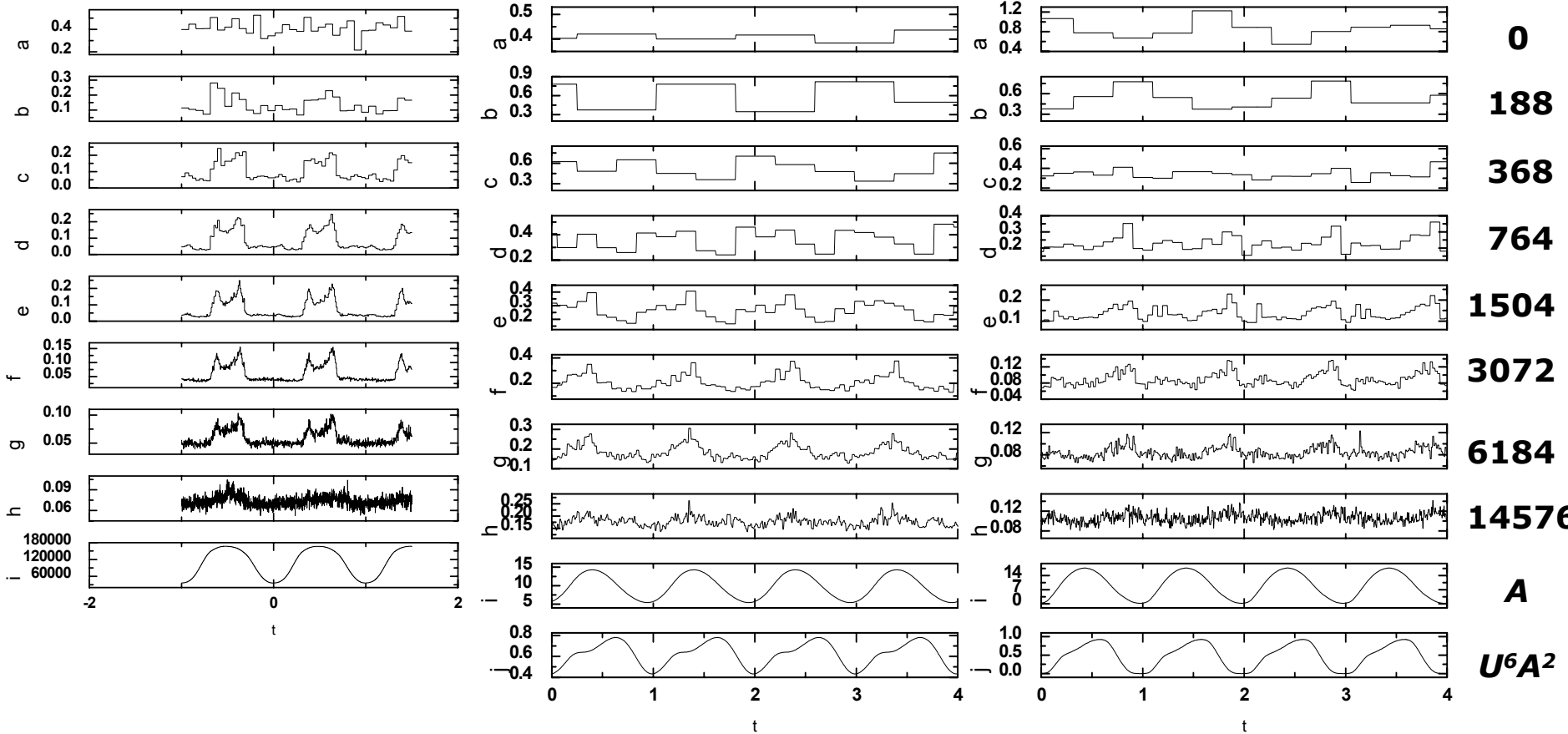
Wavelet Coefficients

**Straight,
20 Hz,
12 cmH₂O**

**Divergent,
200 Hz,
12 cmH₂O**

**Convergent,
200 Hz,
12 cmH₂O**

Hz

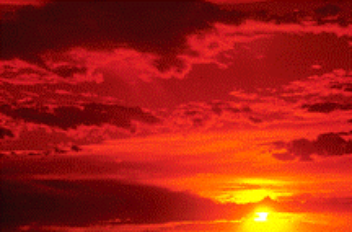


Summary

- **Turbulent sound synchronous with modulation of orifice area**
- **Two peaks during one cycle:**
 - first peak may be associated with the developing of the jet
 - second peak associated with the quenching of the flow during closure.
- **First peak less apparent for high-frequency component**
- **For same level of details, first peak becomes less apparent as the driving frequency increases**

Conclusions

- **quasi-steady approximation verified in confined jets for tonal sound component across various flow conditions, orifice geometries, and acoustic loads**
- **non-stationary broadband investigated using PDF comparisons and wavelet analysis**
- **broadband sound generation appears to be non-stationary (not quasi-steady)**



Ongoing Work

Validation of quasi-steady assumption

- Coanda Effect
- Complex geometries (pathological)

Acoustic scaling laws

- Tonal and broadband
- Evaluate impact on articulatory speech synthesis

Adina Simulations



For more ...

Zhaoyan Zhang, “Experimental study of sound generation by confined jets with application to human phonation,” Ph.D. Dissertation, Purdue University, 2002.

Cheng Zhang, “_____,” M.S.M.E. Thesis, Purdue University, 2002.

Wei Zhao, “A numerical investigation of sound generated from subsonic jets with application to human phonation,” Ph.D. Thesis, Purdue University, 2000.